

The quiescent state of the neutron-star X-ray transient GRS 1747–312 in the globular cluster Terzan 6

Smriti Vats^{1, *}, Rudy Wijnands¹, Aastha S. Parikh¹, Laura Ootes¹, Nathalie Degenaar¹, Dany Page²

¹ Anton Pannekoek Institute for Astronomy, University of Amsterdam, Science Park 904, 1098 XH Amsterdam, The Netherlands

² Instituto de Astronomía, Universidad Nacional Autónoma de México, Mexico D.F. 04510, Mexico

Accepted XXX. Received YYY; in original form ZZZ

ABSTRACT

We studied the transient neutron-star low-mass X-ray binary GRS 1747–312, located in the globular cluster Terzan 6, in its quiescent state after its outburst in August 2004, using an archival *XMM-Newton* observation. A source was detected in this cluster and its X-ray spectrum can be fitted with the combination of a soft, neutron-star atmosphere model and a hard, power-law model. Both contributed roughly equally to the observed 0.5–10 keV luminosity ($\sim 4.8 \times 10^{33}$ erg s⁻¹). This type of X-ray spectrum is typically observed for quiescent neutron-star X-ray transients that are perhaps accreting in quiescence at very low rates. Therefore, if this X-ray source is the quiescent counterpart of GRS 1747–312, then this source is also accreting at low levels in-between outbursts. Since source confusion a likely problem in globular clusters, it is quite possible that part, if not all, of the emission we observed is not related to GRS 1747–312, and is instead associated with another source or conglomeration of sources in the cluster. Currently, it is not possible to determine exactly which part of the emission truly originates from GRS 1747–312, and a *Chandra* observation (when no source is in outburst in Terzan 6) is needed to be conclusive. Assuming that the detected emission is due to GRS 1747–312, we discuss the observed results in the context of what is known about other quiescent systems. We also investigated the thermal evolution of the neutron-star in GRS 1747–312, and inferred that GRS 1747–312 can be considered a typical quiescent system under our assumptions.

Key words: stars: neutron – X-rays: binaries – X-rays: individual: GRS 1747–312

1 INTRODUCTION

Low-mass X-ray binaries (LMXBs) are binary systems harbouring a primary compact accretor (i.e., black hole or neutron-star) and a secondary donor, which is typically a normal star with mass $M \lesssim 1 M_{\odot}$. Mass transfer from the donor occurs via Roche-lobe overflow. The matter forms an accretion disk around the primary star before it is accreted onto the compact accretor. It is this accretion that leads to the observed X-ray emission in these systems (see, e.g., the review chapters in Lewin et al. 1997; Lewin & van der Klis 2010, for more information about X-ray binaries).

Several tens of LMXBs are persistent sources, which means that they are always accreting at relatively high accretion rates (typically producing X-ray luminosities of $L_X > 10^{35-39}$ erg s⁻¹), making them easy to detect and

study with currently available X-ray telescopes. However, most systems are what we call transient LMXBs (or X-ray transients) that are typically very faint (i.e., they are in quiescence) but occasionally exhibit bright X-ray outbursts. These outbursts are due to a sudden, large increase in the rate of accretion onto the compact accretor, causing a similarly large increase in their X-ray luminosities. Transient LMXBs go into outbursts for periods lasting typically from weeks up to months, although in some rare cases these outbursts can last years up to even several decades. During their outbursts the transients can reach X-ray luminosities of $L_X \sim 10^{35-39}$ erg s⁻¹, which is very similar to what is observed from the persistent LMXBs (in outburst the transients indeed look very similar to the persistent systems in many aspects). During quiescence, these systems either accrete at a very low level or they do not accrete at all, and have X-ray luminosities of $L_X \sim 10^{30-34}$ erg s⁻¹.

* E-mail: s.vats@uva.nl

When neutron-star X-ray transients (for a review of

such systems, see [Campana et al. 1998](#)) are in their quiescent state, their X-ray spectra in the 0.5–10 keV energy range can typically have two components (although with a large variety in relative strengths): a soft black-body like component dominating the spectra below 1–2 keV, and a hard power-law shaped component at higher energies (e.g., see [Asai et al. 1996, 1998](#); [Rutledge et al. 2001a,b, 2002a](#), and the articles referencing these papers). The soft spectral component can be attributed to thermal radiation that very likely originates from the surface of the neutron-star. This radiation could be due to the heat generated by accretion onto the surface at very low rates (e.g. [Zampieri et al. 1995](#)), or due to internal heat from the neutron-star itself that is released at the surface (e.g. [Brown et al. 1998](#)). The power-law component of a quiescent neutron-star LMXB may originate from residual accretion of matter onto the neutron-star surface or magnetosphere, however, currently our understanding of this component is inadequate (see the discussions in, e.g., [Campana et al. 1998](#); [Degenaar et al. 2012](#); [Chakrabarty et al. 2014](#)).

During an outburst, the accreted matter compresses the neutron-star crust and heats it up through a set of nuclear reactions (viz. electron captures, neutron emissions, and pycnonuclear reactions), resulting in the release of ~ 1 –2 MeV of energy per accreted nucleon ([Sato 1979](#); [Haensel & Zdunik 1990, 2003, 2008](#); [Steiner 2012](#)). The heat generated by these reactions typically flows into the core, with a small fraction also transported upwards to the surface ([Brown et al. 1998](#)). Due to these processes, the crust and the core go out of thermal equilibrium with one another (if the accretion outburst last for a long period of time – typically many months to years). When the X-ray transient returns back into quiescence, the hot crust cools down by conducting this excess heat to the core and to the surface until it attains thermal equilibrium with the core again ([Rutledge et al. 2002b](#)). Hence, after many repeated accretion episodes, the core too gets significantly heated (e.g., see [Colpi et al. 2001](#); [Wijnands et al. 2013](#)). By studying the heating of the crust, and its subsequent cooling, we can investigate the physics at work in the very dense environments of neutron-star crusts (for a recent observational review see [Wijnands et al. 2017](#)). Also, the longer we study a neutron-star LMXB in quiescence, the deeper we are able to probe into its layers. Systems for which such studies are possible typically show quiescent spectra that are dominated by the soft spectral component (e.g., [Cackett et al. 2013b](#); [Degenaar et al. 2013, 2014](#); [Homan et al. 2014](#); [Merritt et al. 2016](#); [Parikh et al. 2017c](#)), although sometimes a significant power-law component is present as well (e.g., [Fridriksson et al. 2010, 2011](#); [Degenaar et al. 2015](#); [Parikh et al. 2017b, 2018](#)).

For systems having a quiescent spectrum almost fully dominated by a hard component (typically fitted with a power-law model with photon index Γ of 1–2; e.g. [Campana et al. 2002](#); [Wijnands et al. 2005](#); [Heinke et al. 2007, 2009](#); [Degenaar et al. 2012](#)), the quiescent emission might arise due to residual accretion onto the neutron-star magnetosphere. Alternatively, the emission might be due to shocks arising from interaction of the pulsar wind (assuming that the radio pulsar mechanism becomes active) with inflowing matter from the companion star. However, despite those tentative interpretations, the origin of the power-law component in these quiescent systems re-

mains rather unclear (for discussions see [Campana et al. 1998](#); [Degenaar et al. 2012](#); [Degenaar & Wijnands 2012](#)).

There also exist a group of systems where the soft and hard components contribute nearly equally to the quiescent spectrum (typically measured in the 0.5–10 keV energy range). In such cases as well, the origin of the power-law component is not fully understood. Moreover, it is unclear if this power-law component is due to the same mechanisms as the one seen for the power-law dominated systems or if it is due to different processes. However, recent evidence suggests that in sources where both soft and hard components are nearly equally strong, both may be occurring because of low-level accretion onto the neutron-star surface ([Chakrabarty et al. 2014](#); [D’Angelo et al. 2015](#); [Wijnands et al. 2015](#)).

1.1 GRS 1747–312

GRS 1747–312 is a transient LMXB in the globular cluster Terzan 6. It was first discovered in 1990 with the ART-P instrument on-board *Granat* ([Pavlinisky et al. 1994](#)) and with *ROSAT* ([Predehl et al. 1991](#)). The source is located at $\alpha_{J2000} = 17^h 50^m 46.862^s$ and $\delta_{J2000} = -31^\circ 16' 28''.86$, with a 95% error radius of $0''.4$. This position was obtained by [in ’t Zand et al. \(2003\)](#) using an archival *Chandra* observation (ObsID 720) of the source in outburst. The discovery of type-I X-ray bursts from GRS 1747–312 demonstrated that the accretor in this system is a neutron star ([in ’t Zand et al. 2003](#)). This source is quite remarkable in the fact that its outbursts recur very often (see, e.g., [Fig. 1](#)) – with an average recurrence time of 136 days – and has similar outburst behaviour during all observed outbursts ([in ’t Zand et al. 2003](#); [Simon 2009](#)). There are only a handful of other sources that exhibit similar behaviour, with the best known being the Rapid Burster in the globular cluster Liller 1 (e.g., [Masetti 2002](#); [Simon 2008](#)), Aql X-1 (e.g., [Maitra & Bailyn 2008](#); [Campana et al. 2013](#); [Güngör et al. 2014](#)), and H 1743–322 (e.g., [Altamirano & Strohmayer 2012](#); [Zhou et al. 2013](#); a black-hole transient that shows very regular outbursts since 2003). GRS 1747–312 is an eclipsing source with an orbital period of ~ 0.5 d ([in ’t Zand et al. 2003](#)).

Terzan 6 was observed using *XMM-Newton* in 2004 when GRS 1747–312 was in quiescence, and the results were reported by [Saji et al. \(2016\)](#) in conjunction with results from observations during its outburst state (using *Suzaku*, *Chandra* and *Swift*). However, they did not consider potential source confusion due to other unrelated sources in Terzan 6 and did not use the standard spectral decomposition (for quiescent neutron-star LMXBs) of the *XMM-Newton* spectrum in their work (they used a “black-body+CompTT” model). In addition, they did not put the quiescent properties of the source (if indeed the emission was due to GRS 1747–312) into the context of quiescent neutron-star LMXBs, and neutron-star crust heating and cooling. Hence, we reexamined the *XMM-Newton* data and discuss the result of this observation in the above mentioned contexts.

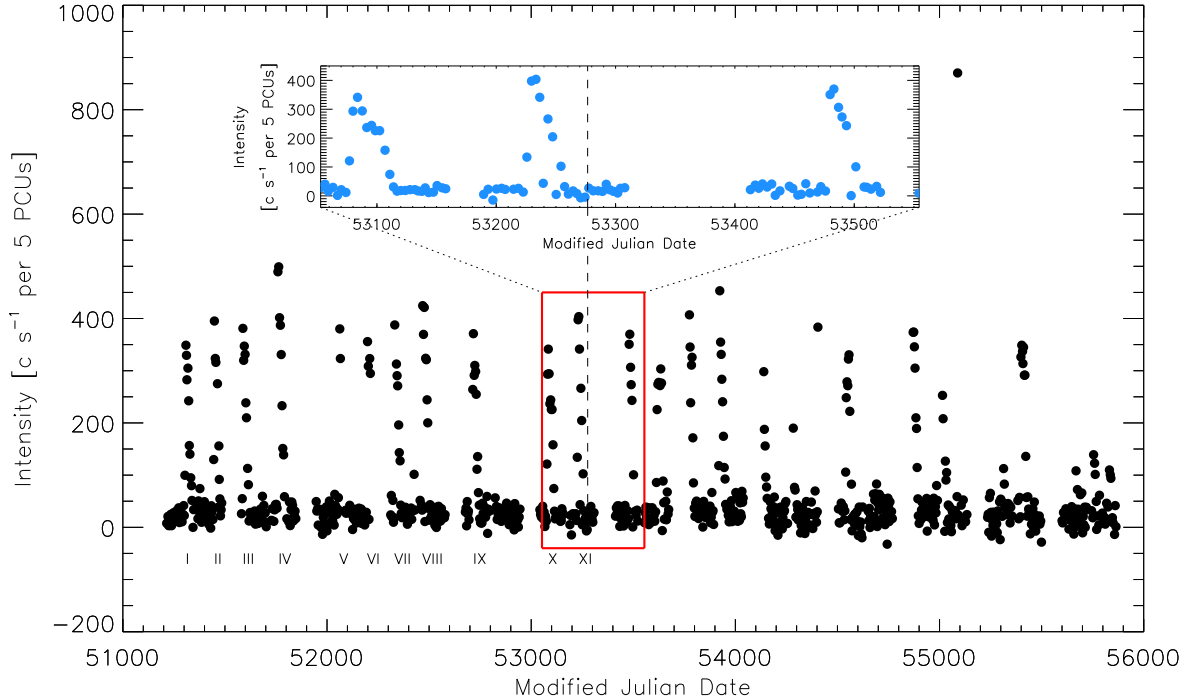


Figure 1. The *RXTE*/PCA (2–60 keV) light curve of GRS 1747–312 obtained between February 1999 and October 2011 as part of the Galactic Bulge Scan program (Swank & Markwardt 2001). The time when the *XMM-Newton* quiescence observation was performed is shown by the dashed line (i.e., it was performed after outburst XI). The roman numbering below the light curve indicates the outbursts that we used to model the thermal evolution of the neutron-star (Sect. 4.3)

2 OBSERVATIONS AND DATA ANALYSIS

GRS 1747–312 was observed on September 28, 2004 using *XMM-Newton* (observation ID: 0206990101) with an exposure time of 8.2 ks for the PN and 14.3 ks each for the MOS detectors. The source was in quiescence during this observation (see Fig. 1; see also Saji et al. 2016) and the data were obtained from the *XMM-Newton* Science Archive¹ (XSA). We reduced the data using the Science Analysis System (SAS; version 15.0.0²) using the standard analysis threads³. Fig. 2 shows the field of view of Terzan 5 with GRS 1747–312 indicated on it.

XMM-Newton collects data using the three EPIC cameras (PN and two MOS detectors), two RGS detectors, and the optical monitor (OM). However the source is too faint to be detected with the RGS, and lies in a crowded globular cluster field, making the optical OM data unavailing. Hence, in this work, we only used data obtained using the MOS1/2 and PN detectors. All EPIC cameras were used in full frame mode, using the medium filter. We processed the raw data using the tools `emproc` and `eproc` for the MOS1/2 and PN detectors, respectively. In order to obtain a data set free of background flaring, we examined the light curves in energies greater than 10 keV for MOS1/2 and be-

tween 10 and 12 keV for PN and used those light curves to determine the parts of the observations during which strong background flares occur. Those intervals were excluded from the data. For MOS1/2 we excluded intervals where the count rate was > 0.15 counts s^{-1} , and for PN where the count rate was > 0.4 counts s^{-1} . The resulting effective exposure times were 12, 11 and 7 ks for the MOS1, MOS2 and PN detectors, respectively.

Since, GRS 1747–312 is an eclipsing source, we investigated if any eclipse occurred during the *XMM* observations. We obtained the ephemeris for the eclipses from in 't Zand et al. (2003), and found that the source did not exhibit an eclipse during the observation.

We extracted the spectra making use of the `xmmselect` tool, using a circular source extraction region (centred on the source position as given by in 't Zand et al. 2003; see also Section 1.1) having a radius of $25''$. Circular background extraction regions were used with radii of $100''$, placed over a source-free part of the CCD on which the source is located. We used the same source region for PN and MOS1/2, but different background regions for each of the detectors (see Figure 2 for the source and background regions for the PN). We used `rmfgen` and `arfgen` to generate the redistribution matrices and ancillary response functions. We grouped the spectra using `specgroup` such that each bin contained a minimum of 15 counts.

To study the long term evolution of the source around the time of the *XMM-Newton* observation, we used the *Rossi*

¹ <https://www.cosmos.esa.int/web/xmm-newton/xsa>

² <https://www.cosmos.esa.int/web/xmm-newton/sas>

³ <https://www.cosmos.esa.int/web/xmm-newton/sas-threads>

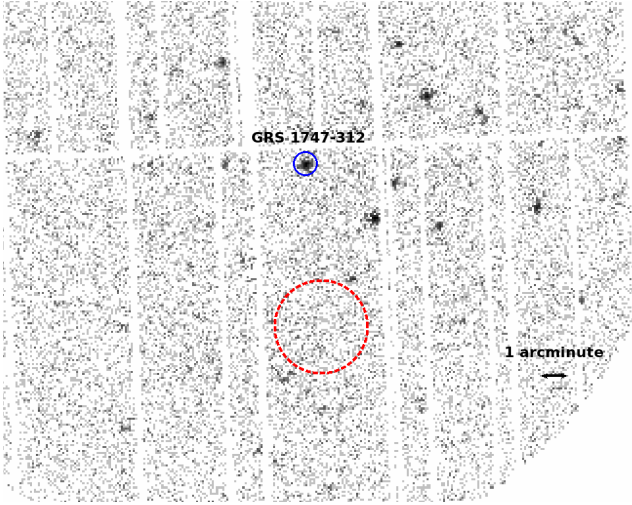


Figure 2. The X-ray image of the field around GRS 1747–312, as obtained using the EPIC-PN camera aboard *XMM-Newton*. The source region is marked with the blue circle with a radius of $25''$ and the background region is marked with the dashed red circle with a radius of $100''$.

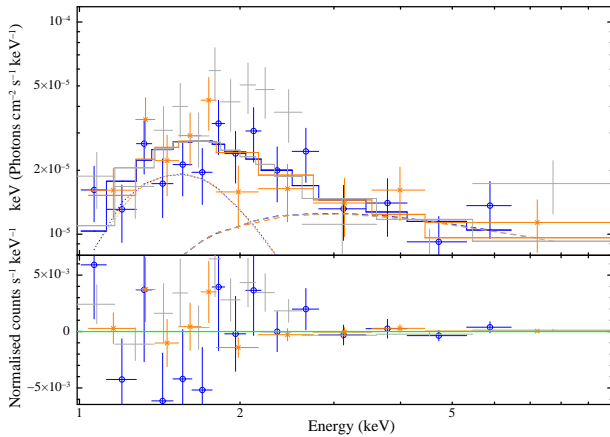


Figure 3. The combined X-ray spectra obtained during the *XMM-Newton* observation – PN(\circ) in blue, MOS1(\times) in orange and MOS2($+$) in grey. Solid lines represent the best fit model for the *XMM-Newton* data; the individual *nsatmos* and *powerlaw* models are represented by dotted and dashed lines respectively. As can be seen, the MOS2 spectrum (grey points) shows an excess of counts at around 2 keV, compared to the PN and MOS1 spectra. The bottom panel shows the fit residuals.

X-ray Timing Explorer (RXTE) Proportional Counter Array (PCA) light curve of the source (see Fig. 1) obtained as part of the Galactic Bulge Scan program⁴ (Swank & Markwardt 2001).

3 RESULTS

The grouped spectra of all three EPIC detectors (MOS1/2 and PN) were fit simultaneously using *XSpec* (version 12.8.1), in the energy range 0.5–10 keV. Since the source

was observed in quiescence (and assuming that the detected emission indeed comes from GRS 1747–312; but see Section 4.1), we first tried to fit the spectra with the commonly used spectral model for quiescent neutron-star LMXBs, viz., a neutron-star atmosphere model (*nsatmos*; Heinke et al. 2006) affected by interstellar absorption modelled using *tbabs*; using WILM abundances (Wilms et al. 2000) and VERN cross-sections (Verner et al. 1996). For the *nsatmos* model, we assumed a neutron-star of mass $1.4 M_{\odot}$ and a radius of 10 km, at a distance of 9.5 kpc (Barbuy et al. 1997; Kuulkers et al. 2003). Also, we assumed that the whole surface of the neutron-star was emitting, so we set the fraction of the surface that is emitting (i.e., normalisation) to 1. This *nsatmos* model assumes that we observe incandescent thermal emission from the neutron-star surface.

However, when using this model we obtained an unsatisfactory fit – $\chi^2/\nu = 3.49$ for 36 degrees of freedom (dof). To improve the fit, we added a power-law component (*XSpec powerlaw* model; also commonly used in modelling quiescent spectra) to the model which resulted in a significant improvement of the fit ($\chi^2/\nu = 1.38$ for 34 dof). We also performed an F-test to determine if the improvement in the fit was a chance occurrence. The probability of a chance occurrence in improvement of the fit is 1.3×10^{-7} , which means that the addition of the power-law component indeed resulted in a model that could explain the spectral shape better. We then included the convolution model *cflux* to obtain the unabsorbed flux contributions (and their errors) for both components in the 0.5–10 keV energy range. We also infer the effective neutron-star temperature as seen by an observer at infinity, kT_{eff}^{∞} ⁵.

In Table 1 we list the obtained spectral parameters. As can be seen from this table the errors on the fit parameters were quite large when leaving all parameters free. This is due to the relatively low number of photons in our spectrum. In order to better constrain some of these parameters, we fitted the same combination of models (*tbabs*, *nsatmos* and *powerlaw*) keeping different combinations of two model parameters fixed, viz., the neutral hydrogen column density to the source, $N_{\text{H}} = 1.4 \times 10^{22} \text{ cm}^{-2}$ (in ’t Zand et al. 2000) and the power law index $\Gamma = 1.5$; a value often found for quiescent neutron-star X-ray transients. Details of the model parameters can be found in Table 1. The obtained neutron-star temperature for the combined *nsatmos* and *powerlaw* model (with the N_{H} free but with the photon index fixed to 1.5, which we roughly find to be the value for our chosen models, as well, if we fixed the N_{H} to $1.4 \times 10^{22} \text{ cm}^{-2}$; see Table 1) was $\sim 112 \text{ eV}$ and the total 0.5–10 keV X-ray luminosity was $\sim 4.8 \times 10^{33} \text{ erg s}^{-1}$ (calculated at a distance of 9.5 kpc). Using this model, we found that the *nsatmos* component contributes $\sim 55.5\%$ and the *powerlaw* contributes $\sim 45.5\%$ to the total (unabsorbed) 0.5–10 keV luminosity.

We found that while the spectra for MOS1 and PN appeared to be consistent with each other, MOS2 showed an excess of counts at around 2 keV (see Figure 3). This effect was observed regardless of the choice of source and background extraction regions. We contacted the *XMM-Newton*

⁵ $kT_{\text{eff}}^{\infty} = kT_{\text{eff}}/(1+z)$, where $(1+z)$ is the gravitational redshift factor, and is equal to 1.31 for our assumed neutron-star of mass $1.4 M_{\odot}$ and radius 10 km.

⁴ <https://asd.gsfc.nasa.gov/Craig.Markwardt/galscan/>

help desk to discuss with them the possibility that the MOS2 data set might be flawed in some way. However, they did not find anything unusual or problematic with this dataset and therefore they concluded that all data could be used. Nonetheless, we repeated the same steps as before whilst fitting only the MOS1 and PN spectra to see what difference it makes to the observed temperature (see Table 1 for the results of these fits as well). For the single *nsatmos* model we obtain a $\chi^2/\nu = 3.65$ for 23 dof, which again was not an acceptable fit. The combination of a *nsatmos* and *powerlaw* model results in an improvement of the fit ($\chi^2/\nu = 0.83$ for 21 dof), which is corroborated by the F-test results (probability of chance occurrence = 1.7×10^{-7}). For this model, we fixed the photon index to 1.5, as the data quality does not allow to meaningfully constrain all spectral parameters independently (see Table 1). As can be seen in Table 1, exclusion of MOS2 data from the spectral fitting leads to a lower inferred neutron-star surface temperature (kT_{eff}^{∞}).

4 DISCUSSION

Here we presented an archival *XMM-Newton* observation performed on the globular cluster Terzan 6 at a time when the transient neutron-star LMXB, GRS 1747–312, was in its quiescent state. This observation was previously reported by Saji et al. (2016). However, they assumed that the source they detected was in fact the quiescent counterpart of this transient, and did not consider the possibility that unrelated cluster sources could have contributed part, or even most, of the observed emission. In addition, they modelled the obtained X-ray spectrum with a two component model (i.e., a black-body plus the *CompTT* model) that are typically not used for quiescent neutron-star X-ray transients. In order to better understand the quiescent properties of GRS 1747–312 we have reanalysed these data.

We confirmed that the spectrum cannot be fitted with a single component model, so as a final spectral model we used a neutron-star atmosphere model (*nsatmos*), combined with a power-law component (*powerlaw*). We obtained a neutron-star temperature of ~ 112 eV and total 0.5–10 keV X-ray luminosity of $\sim 4.8 \times 10^{33}$ erg s $^{-1}$, with both spectral components contributing roughly equally to the total 0.5–10 keV luminosity. All these results are similar to what is frequently found for other quiescent neutron-star X-ray transients. Although this suggests that the emission possibly originated from a quiescent neutron-star transient, and potentially from GRS 1747–312, source confusion might be a serious issue. We discuss this possibility in Section 4.1. Even though we cannot conclusively answer what fraction, if any, of the emission originated from the quiescent counterpart of GRS 1747–312, it is interesting to investigate what could be inferred from this observation if in the future (e.g., by using a high angular resolution observation with *Chandra*) it could be proven that indeed GRS 1747–312 dominates the observed flux. Therefore, in the final two sections of our discussion we explicitly assume that all the emission is due to GRS 1747–312, and we discuss the observed properties in the context of the two main explanations for the quiescent spectra of such systems: residual low-level accretion onto the neutron-star (Section 4.2) and cooling emission from a neutron-star that has been

reheated in outburst due to the accretion of matter (Section 4.3).

4.1 Potential source confusion

In many Galactic globular clusters, multiple faint X-ray sources have been found (for a review on this subject see, e.g., Verbunt & Lewin 2006) and often multiple (candidate) quiescent neutron-star X-ray transients are found in a single globular cluster (see, e.g., Heinke et al. 2003, for a detailed study of quiescent transients in globular clusters). Therefore, it is possible that Terzan 6 might harbour several additional such sources, besides GRS 1747–312 as well. Although the *XMM-Newton* position of the detected source in Terzan 6 is fully consistent with that of GRS 1747–312, the spatial resolution of *XMM-Newton* is insufficient to separate potential close-by sources from each other. Therefore, despite the sub-arcsecond accuracy in the position of GRS 1747–312 (obtained using *Chandra* when the source was in outburst; in 't Zand et al. 2003) we cannot conclusively determine if the X-ray source we detected is indeed the true quiescent counterpart of GRS 1747–312.

Formally, we cannot even exclude the possibility that the observed emission comes from multiple sources. In particular, the different components (the hard and soft component) in the observed X-ray spectra could arise from different sources or source populations. However, this situation would give rise to multiple different scenarios. A full discussion of all these potentially scenarios is beyond the scope of the current paper since nothing conclusive can be inferred from that. Since the properties of the observed source (i.e., the two component spectrum in which both components produce roughly half the observed 0.5–10 keV X-ray luminosity, the exact shape of these two components, and the X-ray luminosity itself) are similar to several quiescent neutron-star transients, we think that it is still possible that we see emission from only one source or that it dominates the observed emission. If so, then this source is most likely the quiescent counterpart of a neutron-star X-ray transient and this could very well be GRS 1747–312 since it is a very active X-ray transient. However, potentially it could still be another, yet unknown, system. If it is the latter case, then the next two sections (Sections 4.2 and 4.3) are invalid in context of GRS 1747–312. This source would then be much fainter than we have assumed, and we would have only an upper limit on its true quiescent emission. The neutron-star surface would then be quite cold indicating that despite the frequent outbursts of the source, the neutron-star is not significantly heated when it is accreting. This then would indicate possible enhanced neutrino emission processes that are active in the core, and thus a relatively massive neutron-star (see Colpi et al. 2001, and discussion in Section 4.3).

If the observed X-ray emission is from an unrelated transient located in Terzan 6, we have not yet conclusively seen an outburst from this source. As shown in Figure 1, many outbursts are observed from the direction of Terzan 6 (see also Pavlinsky et al. 1994; in 't Zand et al. 2000, 2003; Saji et al. 2016) and this trend has continued since the last one shown in the figure. Because eclipses at the expected times are seen in the data (e.g., Bahramian et al. 2013, 2016), some of these outbursts were conclusively assigned to GRS 1747–312, although for most of the other outbursts

Table 1. The results obtained from our X-ray spectral analysis

N_{H} (10^{22} cm $^{-2}$)	Flux $_{\text{nsatmos}}^a$ (10^{-13} erg cm $^{-2}$ s $^{-1}$)	kT_{eff}^∞ (eV)	Γ	Flux $_{\text{powerlaw}}^a$ (10^{-13} erg cm $^{-2}$ s $^{-1}$)	χ^2/ν
PN+MOS1+MOS2					
$1.9^{+0.5}_{-0.6}$	3.1 ± 0.4	$118.2^{+9.9}_{-22.6}$	$1.01^{+1.05}_{-1.03}$	1.9 ± 0.3	1.375 (34 dof)
1.4 (fixed)	1.6 ± 0.3	$101.9^{+7.9}_{-41.4}$	$1.6^{+0.8}_{-0.7}$	2.2 ± 0.3	1.403 (35 dof)
1.8 ± 0.4	2.4 ± 0.4	$112.0^{+8.4}_{-10.7}$	1.5(fixed)	2.0 ± 0.3	1.352 (35 dof)
1.4 (fixed)	1.7 ± 0.3	$103.8^{+3.7}_{-4.2}$	1.5(fixed)	2.1 ± 0.3	1.368 (36 dof)
PN+MOS1					
$1.5^{+0.6}_{-1.0}$	1.5 ± 0.4	$101.0^{+17.6}_{-b}$	$1.6^{+0.7}_{-0.9}$	2.3 ± 0.3	0.829 (21 dof)
1.4 (fixed)	1.4 ± 0.3	$99.3^{+8.9}_{-31.0}$	1.6 ± 0.7	2.3 ± 0.3	0.792 (22 dof)
$1.5^{+0.5}_{-0.7}$	1.6 ± 0.4	$102.7^{+11.7}_{-21.7}$	1.5(fixed)	2.2 ± 0.3	0.792 (22 dof)
1.4 (fixed)	1.5 ± 0.3	$100.8^{+4.6}_{-5.7}$	1.5(fixed)	2.2 ± 0.3	0.760 (23 dof)

All reported uncertainties are at the 90% confidence level.

^a The fluxes are unabsorbed fluxes and for the energy range 0.5–10 keV

^b The lower error did not converge

no such observations are available so they could still, in principle, be due to another source. Moreover, [Saji et al. \(2016\)](#) reported on a *Suzaku* observation performed on 2009 September 16. During this observation they found a faint source ($\sim 10^{35}$ erg s $^{-1}$; faint but brighter than in quiescence, indicating transient activity from the direction of Terzan 6) but they did not find an eclipse at the expected time for GRS 1747–312. While they discussed scenarios in which the observed emission could still have originated from GRS 1747–312, they also provided counter arguments and therefore suggested that another source in Terzan 6 was potentially responsible for this faint emission. However, so far there is no conclusive evidence for an outburst from Terzan 6 that cannot be associated with GRS 1747–312, although we cannot exclude that scenario either. So if the detected flux during the *XMM-Newton* observation indeed comes from a different source, this source has very infrequent and/or very weak outbursts (below the detectability of all-sky monitors or the PCA instrument).

4.2 Residual accretion

Several neutron-star transients have shown similar quiescent spectra as the one we have potentially observed for GRS 1747–312 (e.g. [Fridriksson et al. 2010, 2011](#); [Degenaar et al. 2011, 2015](#); [Waterhouse et al. 2016](#)) i.e., spectra in which the soft and hard component roughly contribute equally to the 0.5–10 keV luminosity. The exact origin of both components was for a long time not fully understood (see, e.g., the discussions in [Degenaar et al. 2015](#)). Variability in the soft component (e.g. Cen X-4, Aql X-1; [Campana et al. 1997, 2004](#); [Rutledge et al. 2002a](#); [Cackett et al. 2010, 2011, 2013a](#); [Bernardini et al. 2013](#)) ruled out that the soft component was due to cooling of the neutron-star crust that is heated during outburst. Therefore, the soft component was often inferred to be due to low-level accretion onto the neutron-star surface (e.g., [Campana et al. 1998, 2004](#); [Rutledge et al. 2002a](#); [Bernardini et al. 2013](#)). The nature of the hard component remained elusive for many years although it had been speculated that this com-

ponent (in addition to the soft component) could also be due to residual accretion onto the neutron-star surface (e.g., see discussion in [Cackett et al. 2010](#)).

Recently the situation has become more clear. [Chakrabarty et al. \(2014\)](#) reported on a simultaneous *XMM-Newton*/*NuSTAR* observation of the quiescent neutron-star system Cen X-4 which showed that the hard component cuts-off at relatively low energies (~ 18 keV) and that this component was best described by a thermal Bremsstrahlung model. They suggested that this component could be due to emission from a hot layer just above the neutron-star surface or from a radiatively inefficient accretion flow. However, [D’Angelo et al. \(2015\)](#) argued that the emission could not come from such a flow but that it had to come from this boundary layer above the neutron-star surface.

In addition, [Wijnands et al. \(2015\)](#) studied the X-ray spectra of neutron-star LMXBs that were accreting at low levels (with luminosities of 10^{34-35} erg s $^{-1}$), but still higher than what is observed in quiescence (when they have luminosities $< 10^{34}$ erg s $^{-1}$). They noted a striking resemblance between the shape of the spectra of the quiescent systems with the systems they studied, i.e., both spectra could be described by a soft plus a hard component, and in both spectra these two components contributed roughly half to the total 0.5–10 keV luminosity. Since for systems with a luminosity of 10^{34-35} erg s $^{-1}$ it is clear that both components have to come from some kind of accretion process, [Wijnands et al. \(2015\)](#) suggested that this would therefore also be true for the quiescent systems that have similar two component spectra. In addition, since both components contribute roughly equally to the emission in the 0.5–10 keV energy band over a large luminosity range of 10^{32} to 10^{35} erg s $^{-1}$ (when taking into account both quiescent and weakly accreting systems), [Wijnands et al. \(2015\)](#) argued that the physical mechanisms behind both components are closely linked to each other (see also [Cackett et al. 2010](#)), and very likely they originate very close to each other. They suggested that the energy stored in the accretion flow is liberated in such a way that half of this energy is released very close to the neutron-star (producing

the hard component through Bremsstrahlung) and the other half when the matter hits the surface (producing the soft, black-body like component). This idea is consistent with the boundary layer picture presented by D’Angelo et al. (2015).

Since the quiescent spectrum of GRS 1747–312 (assuming that it is the origin of all of the emission; see Section 4.1 for caveat) is very similar to the spectra of the systems described in the previous two paragraphs, both in shape and in the way that both components contribute significantly to the 0.5–10 keV luminosity, we suggest that in our source as well, the emission is due to accretion onto the neutron-star (causing surface emission and emission from the boundary layer just above the surface). Previous strong evidence for residual accretion during the quiescent phase of GRS 1747–312 was reported by in ’t Zand et al. (2003), who reported a type-I X-ray burst from this source⁶ when it was in quiescence. In order for this burst to occur, the source must have accreted mass when it was already in quiescence. This burst occurred during a different quiescent interval between two outbursts than when the *XMM-Newton* observation was performed, suggesting that the source is frequently, or perhaps always, accreting at low levels when in quiescence. However, we note that both the quiescent type-I burst as well as the *XMM-Newton* observation occurred relatively close after the end of the preceding outburst (~ 1 month) and therefore, it remains possible that later in quiescence the source stopped fully accreting. If that is true, during a quiescent observation that would be obtained closer in time to the start of the next expected outburst, the source might show a lower quiescent luminosity and potentially also a different type of quiescent spectrum as well. True cooling emission from the neutron-star might be observable (see also Section 4.3) or we might observe a purely power-law dominated spectrum as seen in some other quiescent neutron-star transients. These options can be investigated through a quiescent monitoring campaign of the source after one of its future outbursts, preferably with a high angular resolution telescope like *Chandra* to avoid potential source confusion (see Section 4.1).

4.3 Cooling of a reheated neutron-star crust

Although we consider it possible that the quiescent emission we detected is potentially contaminated (both the soft and hard component could be affected by this) by other sources in Terzan 6 (Section 4.1), it is still interesting to investigate what can be inferred if we assume that the observed soft component was due to cooling of the crust of the neutron-star in GRS 1747–312 that was heated in outburst. Moreover, if during the outbursts the crust is significantly heated

and thus has gone out of thermal equilibrium with the core, the crust might not have relaxed back to thermal equilibrium before the start of the next outburst. This would make the source very similar to Aql X-1 for which we recently investigated this possibility (Ootes et al. 2018). Therefore, it would be interesting to compare our result for GRS 1747–312 with those we obtained for Aql X-1. Although we note that the recurrence times of GRS 1747–312 are similar to those of Aql X-1, GRS 1747–312 has shorter outbursts with lower accretion rates compared to Aql X-1, so the influence of the accretion history might be smaller.

To investigate the evolution of the thermal state of the neutron-star in GRS 1747–312, we have used our updated crust cooling code *NSCool* (Page & Reddy 2013; Page 2016; Ootes et al. 2016) that takes into account accretion rate variability during the multiple outbursts of the source (using the method outlined by Ootes et al. 2018) to determine what we can infer about the neutron-star crust and core for our source. We modelled the full accretion rate history observed between modified Julian dates (MJDs) of 51300 (start of first outburst) and 53474 (end of the quiescent episode during which the *XMM-Newton* observation was performed⁷), based on the observed *RXTE*/PCA bulge-scan light curve (see Fig 1). In this period, eleven accretion outbursts and quiescence episodes were observed, and the *XMM* observation was taken in the quiescence period after the eleventh outburst.

In order to obtain the conversion factor for calculating the bolometric flux, we determined the maximum PCA count rate measured during each of the eleven outbursts and then obtained the mean peak count rate. We found it to be $389.9 \text{ counts s}^{-1}$ per 5 PCUs. in ’t Zand et al. (2000) obtained a *BeppoSAX* observation (using its narrow-field-instruments) during the peak of an outburst of the source and found a unabsorbed flux (0.1–200 keV) of $10.4 \times 10^{-10} \text{ erg cm}^{-2} \text{ s}^{-1}$ (see their Table 1). Assuming that this is a good approximation of the bolometric flux and that the peak flux during each outburst is roughly similar, we obtained (using the averaged PCA peak count rates) a conversion factor of $2.7 \times 10^{-12} \text{ erg cm}^{-2} \text{ s}^{-1}$ per 1 counts s^{-1} for 5 PCUs. We used this factor to convert the observed PCA count rates into bolometric fluxes and subsequently calculate a time-dependent accretion rate which is used as input for the cooling code (see Ootes et al. 2018, for more details about the model).

For each outburst, the start and end time of the outburst were estimated manually (see Table 2). To obtain the start times, we linearly extrapolated the count rates starting at the peak count rate through the data point before the peak. The start times are the times at which this extrapolation reaches zero counts s^{-1} . The end times were determined to be identical to the time of the first quiescent data point. At the end of outburst VI the source became Sun-constrained and hence we have no observations when the quiescent period started. Therefore, we consider the end of this outburst to be 38.33 day after the start of the outburst

⁶ While the type-I burst reported by in ’t Zand et al. (2003) most likely originated from a source in Terzan 6, it is not conclusively certain that this source was indeed GRS 1747–312, and not another, unrelated, quiescent neutron-star X-ray binary in the same cluster (see Section 4.1 for a discussion about potential source confusion). In this paragraph we assume that GRS 1747–312 was indeed the source exhibiting this burst. However, if another source exhibited this type-I X-ray burst, then most of the inferences made in this paragraph about the behaviour of GRS 1747–312 might then instead be applicable to this other source (i.e. if the quiescent emission we observed during the *XMM-Newton* observation also would have come fully from this other source.)

⁷ We did not model the history further because we are only interested in how the previous outbursts of the source would effect the state of the neutron-star during the *XMM-Newton* observation.

(38.33 days is the mean duration of the other fully sampled outbursts).

The accretion rate was determined using

$$\dot{M} = \frac{F_{\text{bol}} 4\pi D^2}{\eta c^2} \quad (1)$$

where F_{bol} is the bolometric flux, $D=9.5$ kpc is the distance to the neutron-star, $\eta=0.2$ is the fraction of the accreted mass that is converted to X-ray luminosity and c is the speed of light. The average accretion rate for the 11 outbursts and quiescence episodes was found to be $\sim 6.6 \times 10^{15} \text{ g s}^{-1}$, which is equal to $\sim 1 \times 10^{-10} M_{\odot}$ per year.

To model the thermal evolution of the source, we assumed that the crustal parameters do not change between outbursts. Although this is likely not realistic for all parameters (e.g., see the studies of [Deibel et al. 2015](#); [Parikh et al. 2017a](#); [Ootes et al. 2018](#)), the data (i.e., only one observational data point) are insufficient to take variations of these parameters into account. For consistency, we used the same mass and radius in our cooling model as used during the spectral fitting ($M=1.4M_{\odot}$, $R=10$ km).

The remaining free parameters in our modelling were the core temperature (T_0), envelope composition (y_{light}), shallow heating depth (ρ_{sh}) and strength (Q_{sh}), and impurity parameters (Q_{imp}). Unfortunately, these parameters are degenerate with each other and with only one observation in quiescence we cannot firmly constrain any of these. One of the pressing issues in crust cooling research is that of the shallow heating phenomenon that is required to explain part of the sources in which crust cooling after an accretion outburst is observed (see, e.g., [Wijnands et al. 2017](#) for a review). We therefore set out to investigate whether or not it is likely that (significant) shallow heating occurs in GRS 1747–312 as well, under the assumption that the observed quiescent emission is due to crust cooling.

To this aim we fixed the envelope composition ($y_{\text{light}} = 10^9 \text{ g cm}^{-2}$), impurity parameter ($Q_{\text{imp}} = 1.0$) and the range of the shallow heating depth (between 1 and $5 \times 10^9 \text{ g cm}^{-3}$) to typically obtained values in other sources (e.g., [Brown & Cumming 2009](#); [Page & Reddy 2013](#); [Ootes et al. 2016](#)). We then changed the base level of the calculated cooling curve (the observed temperature when the crust and core are in thermal equilibrium) in steps by adjusting the core temperature accordingly (note that the observed base level depends on both the core temperature and the envelope composition). For each base level we then determined the maximum shallow heating strength that is allowed by our observation. As input surface temperature we used the value obtained when we fixed the power-law photon index to 1.5 (see Table 1). The results of our modelling are summarised in Table 3.

The results show that only if the source has a very high base level (and thus a relatively hot neutron-star core) compared to most of the other crust cooling sources (see Fig. 2 of [Wijnands et al. 2017](#)), the presence of shallow heating can be excluded in the crust cooling scenario. If the source has a base level that is comparable to other crust cooling sources, our quiescence observation allows for a significant amount of shallow heating (1–5 MeV/nucleon) during the accretion outbursts. This value would be consistent with what is typically found in other sources and therefore GRS 1747–312

Table 2. Start (t_{start}) and end times (t_{end}) for each outburst used in our modelling

Outburst	t_{start}	t_{end}
I	51300	51338
II	51444	51478
III	51584	51623
IV	51755	51803
V	52059	52090
VI	52195	52233
VII	52328	52367
VIII	52465	52500
IX	52695	52747
X	53074	53116
XI	53222	53260

Table 3. The results obtained using our *NSCool* model

T_0 (10^8 K)	Base level (eV)	Maximum Q_{sh} (MeV nucleon $^{-1}$)
1.58	~ 120	0
1.43	~ 115	1.05
1.28	~ 110	2.15
1.13	~ 105	3.10
1.00	~ 100	4.00
0.890	~ 95	4.75
0.785	~ 90	5.45

Note: All parameters (including shallow heating strength) are kept constant between the different outbursts. See text for more details and the exact values of these parameters.

might not be an atypical source. However, we stress that this is only valid under the aforementioned assumptions, and that we indeed see emission from a cooling hot neutron-star crust. As we have argued in Section 4.2, this is likely not true, and therefore the crust could be much colder and hence there might be no need for shallow heating at all. This final conclusion would also be true if none of the emission we observed was due to GRS 1747–312 but to some unrelated cluster source (or sources; see Section 4.1) because the neutron-star (core and crust) in GRS 1747–312 could then be also much colder than assumed in this section.

ACKNOWLEDGEMENTS

SV would like to acknowledge support from NOVA (Nederlandse Onderzoekschool Voor Astronomie). RW, AP and LO acknowledge support from a NWO Top Grant, module 1, awarded to RW. ND is supported by an NWO VIDI Grant. DP is supported by Grant No. 240512 from Conacyt CB-2014-1.

REFERENCES

- Altamirano D., Strohmayer T., 2012, *ApJ*, **754**, L23
 Asai K., Dotani T., Mitsuda K., Hoshi R., Vaughan B., Tanaka Y., Inoue H., 1996, *PASJ*, **48**, 257
 Asai K., Dotani T., Hoshi R., Tanaka Y., Robinson C. R., Terada K., 1998, *PASJ*, **50**, 611

- Bahramian A., Heinke C. O., Altamirano D., Sivakoff G. R., Markwardt C., Homan J., Pooley D., 2013, *The Astronomer's Telegram*, [4915](#)
- Bahramian A., Heinke C. O., Sivakoff G. R., Kennea J. A., Wijnands R., Altamirano D., 2016, *The Astronomer's Telegram*, [9072](#)
- Barbuy B., Ortolani S., Bica E., 1997, *A&AS*, **122**, [483](#)
- Bernardini F., Cackett E. M., Brown E. F., D'Angelo C., Degenaar N., Miller J. M., Reynolds M., Wijnands R., 2013, *MNRAS*, **436**, [2465](#)
- Brown E. F., Cumming A., 2009, *ApJ*, **698**, [1020](#)
- Brown E. F., Bildsten L., Rutledge R. E., 1998, *ApJ*, **504**, [L95](#)
- Cackett E. M., Brown E. F., Miller J. M., Wijnands R., 2010, *ApJ*, **720**, [1325](#)
- Cackett E. M., Fridriksson J. K., Homan J., Miller J. M., Wijnands R., 2011, *MNRAS*, **414**, [3006](#)
- Cackett E. M., Brown E. F., Degenaar N., Miller J. M., Reynolds M., Wijnands R., 2013a, *MNRAS*, **433**, [1362](#)
- Cackett E. M., Brown E. F., Cumming A., Degenaar N., Fridriksson J. K., Homan J., Miller J. M., Wijnands R., 2013b, *ApJ*, **774**, [131](#)
- Campana S., Mereghetti S., Stella L., Colpi M., 1997, *A&A*, **324**, [941](#)
- Campana S., Colpi M., Mereghetti S., Stella L., Tavani M., 1998, *A&ARv*, **8**, [279](#)
- Campana S., et al., 2002, *ApJ*, **575**, [L15](#)
- Campana S., Israel G. L., Stella L., Gastaldello F., Mereghetti S., 2004, *ApJ*, **601**, [474](#)
- Campana S., Coti Zelati F., D'Avanzo P., 2013, *MNRAS*, **432**, [1695](#)
- Chakrabarty D., et al., 2014, *ApJ*, **797**, [92](#)
- Colpi M., Geppert U., Page D., Possenti A., 2001, *ApJ*, **548**, [L175](#)
- D'Angelo C. R., Fridriksson J. K., Messenger C., Patruno A., 2015, *MNRAS*, **449**, [2803](#)
- Degenaar N., Wijnands R., 2012, *MNRAS*, **422**, [581](#)
- Degenaar N., et al., 2011, *MNRAS*, **412**, [1409](#)
- Degenaar N., Patruno A., Wijnands R., 2012, *ApJ*, **756**, [148](#)
- Degenaar N., et al., 2013, *ApJ*, **775**, [48](#)
- Degenaar N., et al., 2014, *ApJ*, **791**, [47](#)
- Degenaar N., et al., 2015, *MNRAS*, **451**, [2071](#)
- Deibel A., Cumming A., Brown E. F., Page D., 2015, *ApJ*, **809**, [L31](#)
- Fridriksson J. K., et al., 2010, *ApJ*, **714**, [270](#)
- Fridriksson J. K., et al., 2011, *ApJ*, **736**, [162](#)
- Güngör C., Güver T., Ekşi K. Y., 2014, *MNRAS*, **439**, [2717](#)
- Haensel P., Zdunik J. L., 1990, *A&A*, **227**, [431](#)
- Haensel P., Zdunik J. L., 2003, *A&A*, **404**, [L33](#)
- Haensel P., Zdunik J. L., 2008, *A&A*, **480**, [459](#)
- Heinke C. O., Grindlay J. E., Lugger P. M., Cohn H. N., Edmonds P. D., Lloyd D. A., Cool A. M., 2003, *ApJ*, **598**, [501](#)
- Heinke C. O., Rybicki G. B., Narayan R., Grindlay J. E., 2006, *ApJ*, **644**, [1090](#)
- Heinke C. O., Jonker P. G., Wijnands R., Taam R. E., 2007, *ApJ*, **660**, [1424](#)
- Heinke C. O., Jonker P. G., Wijnands R., Deloye C. J., Taam R. E., 2009, *ApJ*, **691**, [1035](#)
- Homan J., Fridriksson J. K., Wijnands R., Cackett E. M., Degenaar N., Linares M., Lin D., Remillard R. A., 2014, *ApJ*, **795**, [131](#)
- Kuulkers E., den Hartog P. R., in 't Zand J. J. M., Verbunt F. W. M., Harris W. E., Cocchi M., 2003, *A&A*, **399**, [663](#)
- Lewin W., van der Klis M., 2010, *Compact Stellar X-ray Sources*
- Lewin W. H. G., van Paradijs J., van den Heuvel E. P. J., 1997, *X-ray Binaries*
- Maitra D., Bailyn C. D., 2008, *ApJ*, **688**, [537](#)
- Masetti N., 2002, *A&A*, **381**, [L45](#)
- Merritt R. L., et al., 2016, *ApJ*, **833**, [186](#)
- Ootes L. S., Page D., Wijnands R., Degenaar N., 2016, *MNRAS*, **461**, [4400](#)
- Ootes L. S., Wijnands R., Page D., Degenaar N., 2018, Submitted to *MNRAS*; ArXiv e-prints:1802.06081,
- Page D., 2016, NSCool: Neutron star cooling code, *Astrophysics Source Code Library* (ascl:1609.009)
- Page D., Reddy S., 2013, *Physical Review Letters*, **111**, [241102](#)
- Parikh A. S., et al., 2017a, *MNRAS*,
- Parikh A. S., et al., 2017b, *MNRAS*, **466**, [4074](#)
- Parikh A. S., et al., 2017c, *ApJ*, **851**, [L28](#)
- Parikh A. S., Wijnands R., Degenaar N., Ootes L., Page D., 2018, *MNRAS*,
- Pavlinko M. N., Grebenev S. A., Sunyaev R. A., 1994, *ApJ*, **425**, [110](#)
- Predehl P., Hasinger G., Verbunt F., 1991, *A&A*, **246**, [L21](#)
- Rutledge R. E., Bildsten L., Brown E. F., Pavlov G. G., Zavlin V. E., 2001a, *ApJ*, **551**, [921](#)
- Rutledge R. E., Bildsten L., Brown E. F., Pavlov G. G., Zavlin V. E., 2001b, *ApJ*, **559**, [1054](#)
- Rutledge R. E., Bildsten L., Brown E. F., Pavlov G. G., Zavlin V. E., 2002a, *ApJ*, **577**, [346](#)
- Rutledge R. E., Bildsten L., Brown E. F., Pavlov G. G., Zavlin V. E., Ushomirsky G., 2002b, *ApJ*, **580**, [413](#)
- Saji S., et al., 2016, *PASJ*, **68**, [S15](#)
- Sato K., 1979, *Progress of Theoretical Physics*, **62**, [957](#)
- Simon V., 2008, *A&A*, **492**, [135](#)
- Steiner A. W., 2012, *Phys. Rev. C*, **85**, [055804](#)
- Swank J., Markwardt C., 2001, in Inoue H., Kunieda H., eds, *Astronomical Society of the Pacific Conference Series Vol. 251, New Century of X-ray Astronomy*. p. 94 ([arXiv:astro-ph/0109240](#))
- Verbunt F., Lewin W. H. G., 2006, *Globular cluster X-ray sources*. pp 341–379
- Verner D. A., Ferland G. J., Korista K. T., Yakovlev D. G., 1996, *ApJ*, **465**, [487](#)
- Waterhouse A. C., Degenaar N., Wijnands R., Brown E. F., Miller J. M., Altamirano D., Linares M., 2016, *MNRAS*, **456**, [4001](#)
- Wijnands R., Heinke C. O., Pooley D., Edmonds P. D., Lewin W. H. G., Grindlay J. E., Jonker P. G., Miller J. M., 2005, *ApJ*, **618**, [883](#)
- Wijnands R., Degenaar N., Page D., 2013, *MNRAS*, **432**, [2366](#)
- Wijnands R., Degenaar N., Armas Padilla M., Altamirano D., Cavecchi Y., Linares M., Bahramian A., Heinke C. O., 2015, *MNRAS*, **454**, [1371](#)
- Wijnands R., Degenaar N., Page D., 2017, *Journal of Astrophysics and Astronomy*, **38**, [49](#)
- Wilms J., Allen A., McCray R., 2000, *ApJ*, **542**, [914](#)
- Zampieri L., Turolla R., Zane S., Treves A., 1995, *ApJ*, **439**, [849](#)
- Zhou J. N., Liu Q. Z., Chen Y. P., Li J., Qu J. L., Zhang S., Gao H. Q., Zhang Z., 2013, *MNRAS*, **431**, [2285](#)
- in 't Zand J. J. M., et al., 2000, *A&A*, **355**, [145](#)
- in 't Zand J. J. M., et al., 2003, *A&A*, **406**, [233](#)
- Šimon V., 2009, *New Astron.*, **14**, [443](#)

This paper has been typeset from a $\text{\TeX}/\text{\LaTeX}$ file prepared by the author.